

Time-lapse Seismic Analysis Using Well Logs, White Rose Field

Ying Zou and Laurence R. Bentley - University of Calgary

CSEG Geophysics 2002

Summary

In order to understand the changes of reservoir conditions with the stages of production we need to link reservoir properties to 4-D seismic survey which covers the entire reservoir volume between the wells. This work demonstrates a method to model time-lapse seismic responses due to fluid substitution. It is based on sonic logs and density logs before production. Three scenarios are presented, i.e. gas drive, water drive and gas/water drive. Using PVT data and inferred post-production saturation, new sonic logs and density logs are generated. Synthetic seismic and AVO models are compared before and after production for a case study in White Rose Field. Reflection coefficients at the gas-oil contact (GOC) and the oil-water contact (OWC) change in magnitude approximately 15%. The synthetics indicate that P-P and P-S AVO responses can be used to observe the changes in fluid distributions. The change in density due to fluid substitution appears to be the major factor in changing the seismic response. The synthetic time-lapse seismic response analysis can be effective tools in 4-D seismic feasibility study.

Introduction

Time-lapse seismic surveys have been used to monitor reservoir changes due to production. Time-lapse seismic monitoring of reservoirs is based on changing seismic response due to fluid substitution and pressure changes. The observable changes in seismic response can help locate bypassed oil, water- or gas-flood fronts and heat flow (Sonneland et al, 1997). We also know that there are risks associated with a 4-D seismic project include false anomalies caused by acquisition, processing and the ambiguity of seismic interpretation in relating the seismic changes to the reservoir changes. Lumley et al (1998) proposed a four step feasibility and risk assessment study before undertaking a 4D seismic project. The proposed third step is the seismic modeling from sonic and density logs. This study demonstrates a procedure for the modeling of time-lapse seismic from time-lapse well logs. Three scenarios are assumed for the possible field conditions. A methodology is developed for the calculation of the seismic response based on the Gassmann equation and a modification of the procedure described by Bentley et al. (2000).

Theory and Methodology

A brief description of the procedure is presented here plus some revisions to the original scheme (Bentley et al. 2000). The Gassmann's equation relates the bulk modulus of a saturated rock (K_u), to the dry rock bulk modulus (K_d), the solid grain modulus (K_s), the fluid bulk modulus (K_f) and the porosity ϕ (Wang and Nur, 1992),

$$K_u = K_d + \frac{(1 - K_d / K_s)^2}{\frac{\phi}{K_f} + \frac{1 - \phi}{K_s} - \frac{K_d}{K_s^2}} \quad (1)$$

Density is calculated as following,

$$\rho_f = S_g \rho_g + S_o \rho_o + S_w \rho_w \quad (2)$$

$$\rho_o = \frac{\rho_o^{std} + R_s \rho_g^{std}}{B_o} \quad (3)$$

$$\rho_u = \rho_s (1 - \phi) + \rho_f \phi \quad (4)$$

where $\rho_o, \rho_g, \rho_w, \rho_s, \rho_u, \rho_f$ are the densities of oil, gas, water, solid grains, saturated reservoir rock and fluid mixture at reservoir condition. And ρ^{std} is the density of oil or gas at standard conditions. R_s is the gas oil ratio and B_o is the oil formation volume factor. The equations of Batzle and Wang (1992) are used to calculate ρ_g, K_g, ρ_w and K_w (adiabatic) using the known reservoir pressure, temperature, gas specific gravity and water salinity. From (2) and (3) we obtain ρ_f and from (4) we can get undrained rock density ρ_u . We can get ϕ, ρ_s and K_s from core test. Using the empirical equations developed by Vasquez and Beggs (1980) C_o ($K_o = 1/C_o$) can be calculated if we know the specific gravity of gas, separator pressure and temperature, and oil API gravity. The fluid mixture bulk modulus has the limiting values (Biondi et al., 1998),

$$\frac{1}{K_{f1}} = \frac{S_g}{K_g} + \frac{S_o}{K_o} + \frac{S_w}{K_w} \quad (5)$$

$$K_{f2} = S_g K_g + S_o K_o + S_w K_w \quad (6)$$

Equation (5) is for homogeneous fluid distribution and Equation (6) is for patchy fluid distribution. We take an average of these two to get K_f . The undrained bulk and shear moduli are computed from P- and S-velocity, and density logs using $\underline{K}_u = \rho_u (V_p^2 - 4/3V_s^2)$ and $\mu_u = \rho_u V_s^2$. K_d can be calculated from K_u , the porosity, a given value of K_s and an estimate of K_f through the Gassman equation. New reservoir pressure, temperature and saturations are specified by the analyst. Gas, oil and water bulk moduli and densities are computed using the equations of

Batzle and Wang (1992). By equations (2) and (4), the new fluid density, the new fluid saturation, the porosity and the solid grain density are used to calculate the new undrained bulk density. The percentage change in undrained bulk density is calculated using the new and old calculated undrained bulk densities. The original density logs are multiplied by the percentage change to generate an updated density log. The updated values can be used with the Gassman equation to update the undrained bulk modulus. These are then used to update the velocity logs. We developed a Matlab program to calculate sonic and density logs based on the method described above.

A case study

The White Rose field is located in Jeanne d'Arc Basin off shore Newfoundland. Husky Oil drilled the Whiterose L-08 well during the spring of 1999. The geology consists of a thick section of Tertiary shales separated from Cretaceous shales by an unconformity. Gas and oil were discovered in the underlying Cretaceous Avalon sands (Hedlin, 2000). A partial of density log and P-wave log and corridor stack from a down-hole VSP survey is shown in Figure 1. A wavelet was extracted from VSP corridor stack, applied to the original logs and zero offset synthetic traces were generated (Figure 1). Hampson-Russell's STRATA and AVO package are used to tie synthetic traces with corridor stack and to do AVO modeling. It is necessary to point out that the AVO at GOC and OWC in our case is not the conventional AVO. For conventional AVO it means that the reflection is between overlying shale and underlying sands. In this case the reflection at GOC or OWC is from the interface between sands which has different fluid content (gas, oil or water). In oil leg, the average porosity is 0.19, the average connate water is 0.2, reservoir pressure is 29.4 Mpa, reservoir temperature is 106°C, gas oil ratio is 122SCF/STB, oil formation volume factor is 1.37 BBL/STB. The specific gravity of gas is 0.734 and the oil API° is 31. The White Rose Field has not been produced to date. In this study, we investigate the following three drive production scenarios. (1) Gas drive through the whole oil leg. Oil is replaced by gas. Residual oil is 0.3 and connate water is 0.22. (2) Water drive through the whole oil leg. Oil is replaced by water. Residual oil is 0.3 and there is no gas saturation. (3) Half oil leg is replaced by gas and the other half is replaced by water. All scenarios assume that reservoir pressure and temperature are maintained at the initial levels.

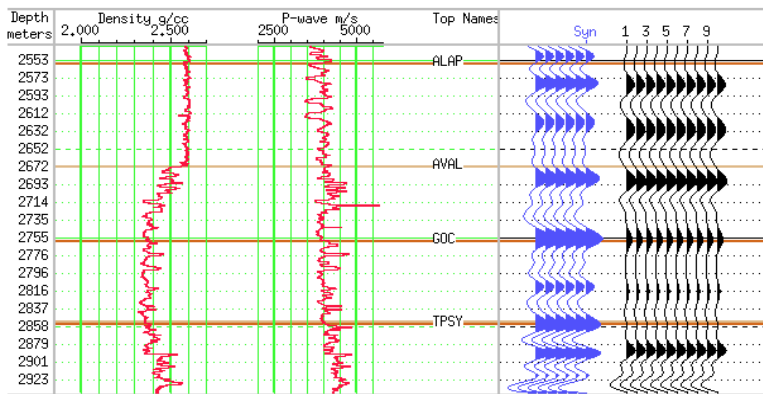


Figure 1. The original logs, the synthetic trace (blue) and the VSP corridor stack (black)

Results discussion

Table 2 and 3 provide a summary of the changes due to fluid substitution. For gas drive, the bulk modulus decreases 2.3 %, but the P wave velocity increases due to a 1.9 % decrease in density. The S wave velocity increases 0.9 %. The velocity changes are small due to the large value of K_d compared to the pore fluid contribution to K_u . For the water drive case, the P wave velocity increases 0.6 %, the S wave average velocity decreases 0.5 % and the average bulk modulus increases 4.4 %. Although the percentage change in density and velocity are small, they lead to changes in the reflection coefficients from the original GOC and OWC on the order of 15%.

Table 2. Mean (M) change, mean percentage change (%), and their standard deviation (std) in oil leg zone due to fluid substitution, gas drive case

Gas drive	$K_u(GP\alpha)$	$\rho_u(Kg/m^3)$	$V_p(m/s)$	$V_s(m/s)$	AIP(Kg/m ² s)
M	-.44	-43.85	15.74	23.64	-148851
std	.14		10.13	1.13	14463.7
%	-2.3	-1.9	.4	.9	-1.5
std	.009		.002	.0001	.002

Table 3. Mean changes (M), mean percentage change (%) and their standard deviation (std) in oil leg zone due to fluid substitution, water drive case

Water drive	$K_u(GP\alpha)$	$\rho_u(Kg/m^3)$	$V_p(m/s)$	$V_s(m/s)$	AIP(Kg/m ² s)
M	0.84	23.56	24.13	-12.43	157414
std	0.26		16.13	0.59	33322.5
%	4.4	1.0	.6	-.5	1.6
std	.017		.004	.0001	.004

The AVO modeling uses Zoeppritz equations in Hampson-Russell's AVO package. Figure 2 compares the AVO effects of the three drive mechanisms with original log case. The fluid substitutions do not change the AVO trend but they do change the AVO amplitudes. The differences between the synthetics due to different drive mechanism are visible. The amplitude at the GOC decreased slightly in gas drive

scenario and increased in water drive scenario. At the OWC the amplitude increased slightly in gas drive scenario and decreased in water drive scenario. Figure 3 gives reflection coefficients for both GOC and OWC using averaged velocity and density over 10 meter interval above and below the interface. It shows that the AVO trends are the same for all scenarios but the zero-offset values are different for each case.

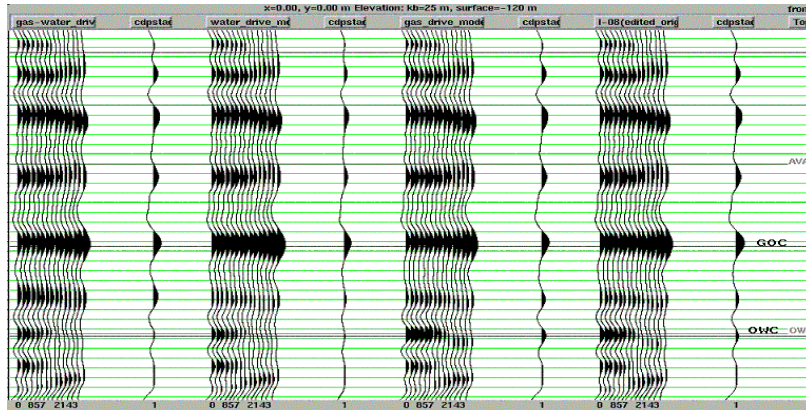


Figure 2. AVO modeling (from left to right) for gas/water, water, gas drive and original logs

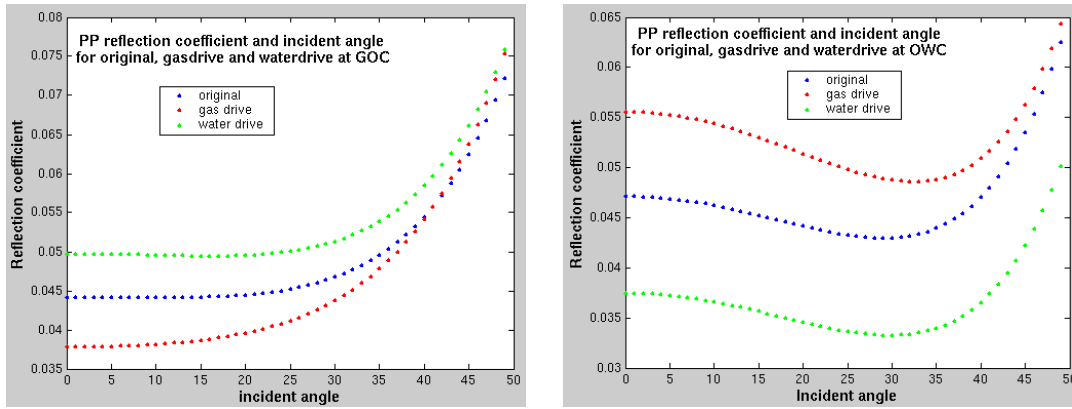


Figure 3. Reflection coefficient changes with incident angle for PP wave

Due to the limited space we only give gas/water drive synthetic plot with 20% noise added (Figure 4). From the difference traces we can see that the largest amplitude difference is at the new GWC, the second largest difference is at the OWC and the smallest difference is at the GOC. It is obvious that the more contrast between original fluid and substitute fluid the larger difference on seismic. We also can notice that the difference AVO gather shows the differences varying with offset slightly.

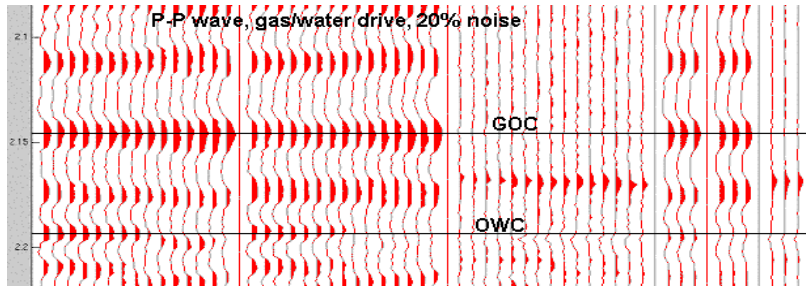


Figure 4. The original and gas/water drive PP gather, their difference, stacked traces and their difference

We also did modeling for P-S converted wave. Figure 5 is the synthetic gathers for original and gas drive case, difference gather and stacked traces. The reflection coefficient for the P-S converted wave (approximation) (Bortfeld, 1961) is:

$$R_{ps} = -\tan \theta_4 \left\{ \left(\frac{V_{p1} + V_{p2}}{V_{s1} + V_{s2}} \right) \left(\frac{\rho_2 - \rho_1}{\rho_2 + \rho_1} \right) + 4 \left[\left(\frac{V_{s2} - V_{s1}}{V_{s2} + V_{s1}} \right) + \frac{1}{2} \left(\frac{\rho_2 - \rho_1}{\rho_2 + \rho_1} \right) \right] \cos(\theta_1 + \theta_4) \right\}$$

Using this equation, the reflection coefficients for the P-S converted wave are calculated and plotted on Figure 6. We see a trend in the P-S reflections of strengthening reflection with offset until a maximum strength is reached followed by decreasing reflection strength. Fluid substitution has changed the position of the maximum amplitude offset from case to case. For water drive the reflection curve is close to the

original case, because shear modulus does not change with water saturation. Therefore, V_s is not sensitive to fluid saturation. For gas saturation case V_s changes mainly because of the density decrease. In the both gas and water drive cases, the P-S wave shows a visible changes in the amplitude in the oil zone. Here we only display the gas drive case because of the limited space.

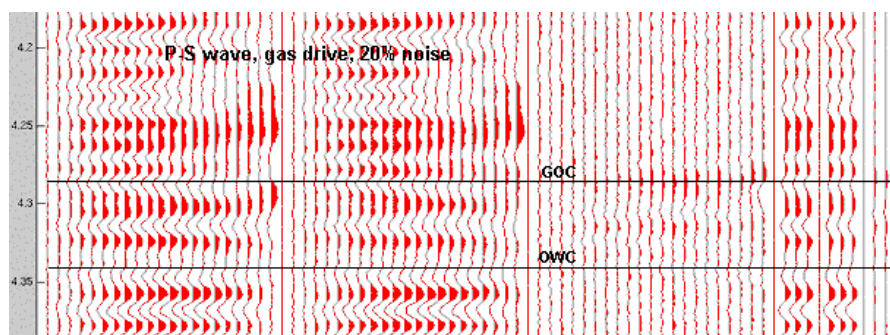


Figure 5. The original and gas drive PS gather, their difference, stacked traces and their difference

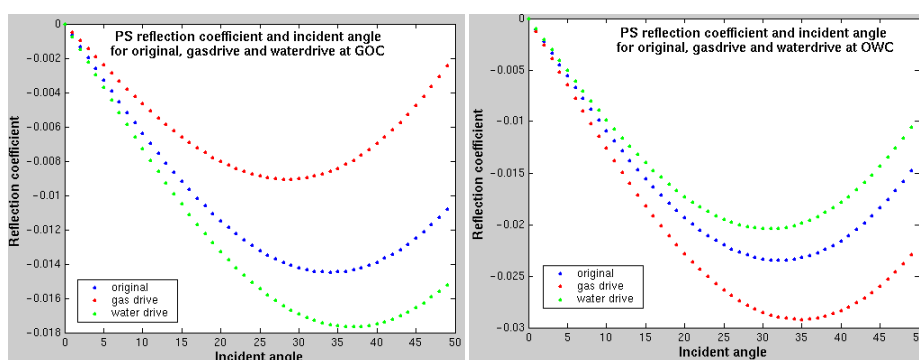


Figure 6. Reflection coefficient changes with incident angle for PS wave

Conclusions

The substitution of reservoir oil by gas and water can cause changes in seismic response and that can be modeled using well logs plus reservoir parameters. Our case study shows that :1). Synthetic modeling results predict that gas or water drives will cause changes of reflection coefficients on the order of 15% at zero offset. The more contrast between original fluid and substitute fluid the larger the difference on seismic traces. 2). The amplitude differences due to fluid substitution on the difference AVO gather change slightly with offset for PP wave and for PS wave the maximum amplitude offset position changes for different fluid saturation. 3). Due to the relatively high value of the dry bulk modulus, K_d , and the moderate porosity, the influence of the fluid saturation changes is relatively small. It appears that most of the change in seismic response is due to the change in acoustic impedance caused by fluid replacement induced changes to the density. 4). AIP changes for both gas drive and water drive are -1.5% and 1.6% , respectively. Although it is visible in synthetic traces, it might be difficult to detect on field data (AIP $<4\%$) according to Lumley et al. (1998). 5). Synthetic time-lapse seismic responses calculated using reservoir data and petrophysical data can be effective tools for feasibility and risk assessment studies.

References

- Batzle, M. and Wang, Z., 1992, Seismic Properties of Pore Fluids: Geophysics, 57,1396-1408.
- Bentley, L. R., J. Zhang and H-X. Lu, 2000, Evaluating feasibility of seismic fluid monitoring, paper RC7,SEG Annual Meeting, Calgary, Aug. 6-11.
- Bortfeld, R., 1961, Approximation to the Reflection and Transmission Coefficients of Plane Longitudinal and Transverse Waves: Geophys. Prosp., 9, 485-503.
- Hedlin, K., 2000, Pore Space Modulus and Extraction Using AVO: SEG GeoCanada 2000 Convention Abstract.
- Lumley, D. E. and Behrens, R. A., 1998, Practical Issues of 4D Seismic Reservoir Monitoring: What an Engineer Needs to Know, SPE Reservoir Evaluation & Engineering, 528-538.
- Sonneland, L., Hafslund Veire, H., Raymond, B., Signer, C., Pederson, L., Ryan, S., and Sayers, C., 1997, Seismic Reservoir Monitoring on Gullfakes: The Leading Edge, 16, No. 9, 1247-1252.
- Vasques, M. and Beggs, H. D., 1980, Correlations for Fluid Physical Property Predictions: JPT, 32, 968-970.
- Wang, Z. and Nur, A., 1992, Elastic Wave Velocities in Porous Media: A theoretical Recipe in Seismic and Acoustic Velocities in Reservoir Rocks: 2 Theoretical and Model Studies, SEG, 1-35.